Nanoscale

PAPER

View Article Online
View Journal | View Issue

Cite this: *Nanoscale*, 2025, **17**, 17769

Strong magnetic exchange coupling of a dibenzo-fused rhomboidal nanographene and its homocoupling with tunable periodicities on a metal surface†

Ana Barragán,[a] Goudappagouda,[b] Manish Kumar,[c,d] Diego Soler-Polo,[d] Elena Pérez-Elvira,[a] Andrés Pinar Solé,[d] Alba García-Frutos,[a] Zhiqiang Gao,[b] Koen Lauwaet,[a] José M. Gallego,[e] Rodolfo Miranda,[a] David Écija,*[a,f] Pavel Jelínek,*[d] Akimitsu Narita*[b] and José I. Urgel*[a,f]

Received 4th March 2025,
Accepted 2nd July 2025

DOI: 10.1039/d5nr00957j

rsc.li/nanoscale

Open-shell nanographenes (NGs), also known as molecular π-magnets, have recently garnered attention for their potential in spintronics and quantum computing. Tailoring of such NGs at the atomic level allows the control of their magnetic interactions. We report here the on-surface synthesis of a dibenzo-fused rhomboidal NG with predominant zigzag edges featuring an open-shell (antiferromagnetic) character and a high value of magnetic exchange coupling (MEC) on Au(111) surfaces. Scanning tunneling microscopy (STM) and noncontact atomic force microscopy (nc-AFM) confirm its chemical structure. Scanning tunneling spectroscopy (STS) measurements, complemented by state-of-the-art theoretical calculations, reveal the open-shell character of the NG, observed as singlet–triplet inelastic excitations. Furthermore, molecular chains consisting of these NGs were fabricated with tunable periodicities through the functionalization of the precursor, showing the absence of MEC between adjacent units, which provides deeper insights into the behavior of open-shell systems and preservation of individual magnetic entities within π-conjugated structures.

Introduction

In recent years, the precise synthesis of open-shell nanographenes (NGs), also known as molecular π-magnets,[1–3] has captured significant attention due to their potential in advancing spintronics and quantum computing.[4] One of the key factors behind this growing interest is the ability to tune the magnetic exchange coupling (MEC) between unpaired electrons in these systems. Strategic designs of molecular precursors enable to tailor their size, shape, and edge topology at the atomic level, providing unprecedented control over their magnetic properties and access to such finely tuned magnetic interactions. In this regard, different approaches have been explored to induce magnetism in NGs, including: (i) sublattice imbalance of the honey-comb bipartite lattice; (ii) topological frustration of both sets of bipartite sublattices; (iii) strong electron–electron correlation to induce spin polarization of frontier orbitals, (iv) introduction of topological defects[5] and length-dependent vibronic coupling between occupied and unoccupied frontier orbitals.[6] In addition to these approaches, a substantial modification of the electronic and magnetic properties in carbon-based nanostructures can be achieved through heteroatom doping.[7]

Nowadays, the combination of on-surface bottom-up synthesis with scanning probe microscopy (SPM) techniques has emerged as a powerful method to achieve such typically unstable NGs under ultra-high vacuum (UHV) conditions. This approach takes advantage of the metal surface stabilization of the NGs, providing an appealing playground for their study and characterization as model π-electron systems.[8] Following the aforementioned concept of topological frustration, the magnetism of the Clar's goblet was recently demonstrated.[9]

[a]*IMDEA Nanoscience, C/Faraday 9, Campus de Cantoblanco, 28049 Madrid, Spain. E-mail: david.ecija@imdea.org, jose-ignacio.urgel@imdea.org*
[b]*Organic and Carbon Nanomaterials Unit, Okinawa Institute of Science and Technology Graduate University, 1919-1 Tancha, Onna-son, Kunigami-gun, Okinawa 904-0495, Japan. E-mail: akimitsu.narita@oist.jp*
[c]*Department of Condensed Matter Physics, Faculty of Mathematics and Physics, Charles University, Prague 2, CZ-12116, Czech Republic*
[d]*Institute of Physics of the Czech Academy of Science, Cukrovarnická 10, 16200 Prague 6, Czech Republic. E-mail: jelinekp@fzu.cz*
[e]*Instituto de Ciencia de Materiales de Madrid (ICMM), CSIC, Cantoblanco, 28049 Madrid, Spain*
[f]*Unidad de Nanomateriales avanzados, Imdea Nanoscience, Unidad asociada al CSIC por el ICMM, 28049 Madrid, Spain*

† Electronic supplementary information (ESI) available. See DOI: https://doi.org/10.1039/d5nr00957j

Since then, theoretically proposed and long-pursued pristine members of several NG families have been synthesized on the Au(111) surface, experimentally demonstrating open-shell diradical characters and different magnetic ordering between unpaired spins. For instance, NGs with a triplet ground state (S = 1) include triangulene and its heteroatom doped derivatives,[10,11] extended triangulenes[12] and heptauthrene,[13] together with several porphyrinoids with phenalenyl π-extensions;[14,15] and those with a singlet ground state (S = 0) peripenta- and periheptacene,[16–18] super-nonazethrene[19] and pentadecacene[20] among others[21–24] (see Scheme 1 for some representative π-magnetic NGs that have been achieved recently). Particularly intriguing has been the recent fabrication of NGs with fused benzene rings arranged in a rhomboidal configuration with predominantly zigzag edges,[25–29] exhibiting record-breaking values of magnetic MEC on the Au(111) surface.[27] Only recently, the study of diradical NGs has been extended to higher polyradical systems[30–36] and related low-dimensional quantum magnets.[37–43] In fact, a high MEC value (higher than the Landauer limit)[44] can be of crucial importance for improving spin transport, state stability, and energy efficiency in futuristic NG-based spintronic devices and quantum computing elements.[45] This can be particularly relevant for systems with minimized interactions between constituting units,[46–48] *i.e.* showing an isolated magnetic behavior without long-range order, allowing for independent manipulation of spin states.

In this work we demonstrate an on-surface synthesis of a dibenzo-fused rhomboid-shaped NG **1** on an Au(111) surface under UHV conditions, which belongs to the family of rhomboid-shaped NGs with strong exchange coupling through a net spin polarization of edge states. Extending the nomenclature of [n]rhombene for zigzag edges of m and n benzene rings [m, n]rhombene, **1** can thus be called dibenzo[5,4]rhombene (see Scheme 1), the structure of which is unambiguously evidenced by scanning tunneling microscopy (STM) and noncontact atomic force microscopy (nc-AFM). Scanning tunnelling spectroscopy (STS), complemented by state-of-the-art theoretical calculations, reveals the electronic and magnetic properties of **1**. This spectroscopic measurements identify the Coulomb gap

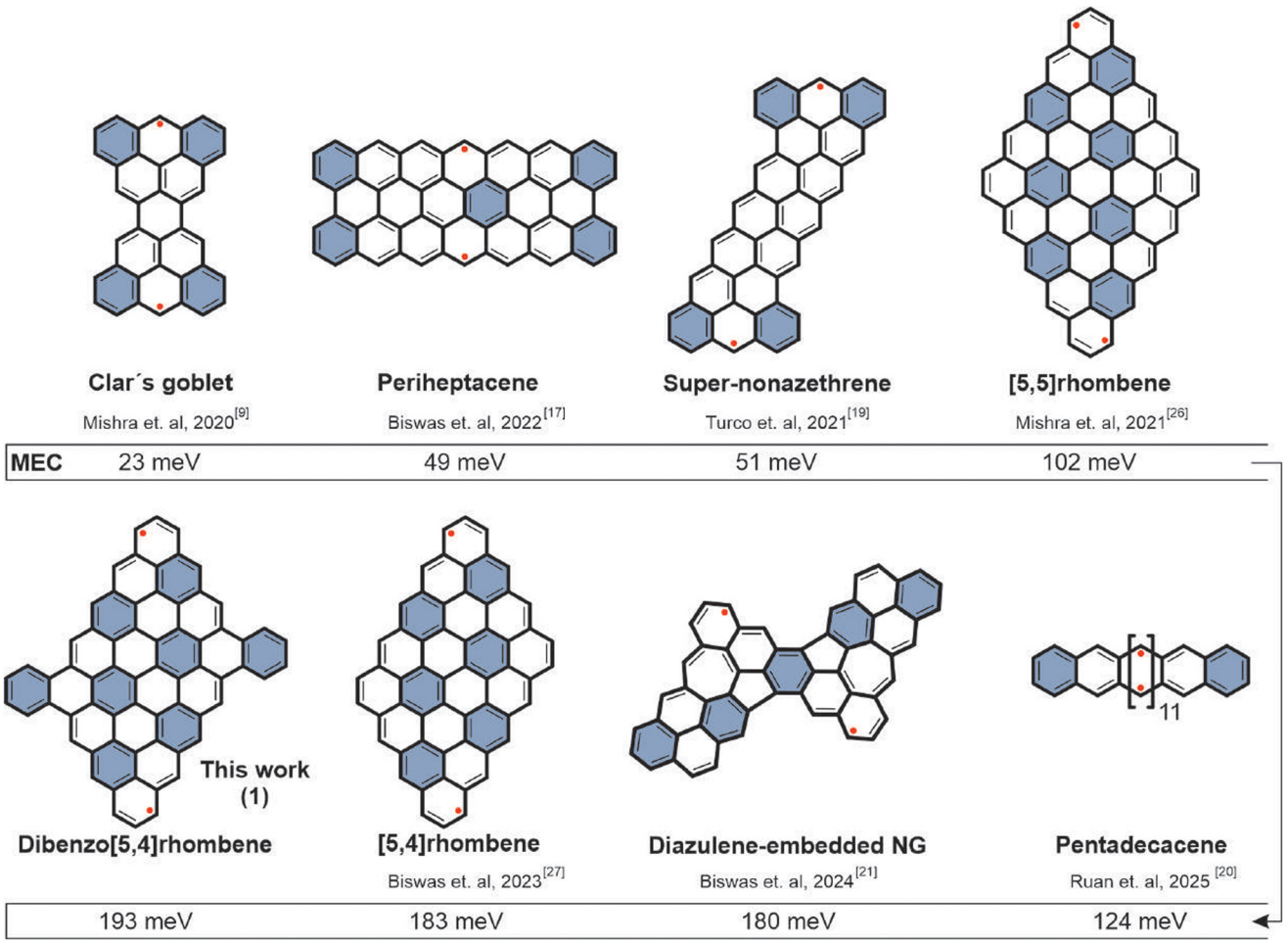

Scheme 1 Representative examples of open-shell singlet nanographenes synthesized on the Au(111) surface. The chemical sketches represent one of the possible diradical non-Kekulé resonance structures for each nanographene, together with the reported MEC found between unpaired spins. Blue filled rings correspond to Clar sextets and red dots to unpaired spins.

and confirms the open-shell character of the NG, preserved on a metallic substrate, as evidenced by singlet–triplet inelastic excitations. Notably, **1** presents an increment in the MEC of ≈10 meV compared to the [5,4]rhombene. Moreover, we demonstrate the fabrication of molecular chains consisting of **1** through the functionalization of the molecular precursor. By installing bromo or isopropyl functional groups for its homocoupling, we achieve the direct conjugation of **1** by intermolecular carbon–carbon coupling (**2**) or by the introduction of a phenylene linker in between (**3**), respectively, enabling tuning of the periodicity of antiferromagnetic units in the resulting chains. Herein, we observed the lack of MEC between adjacent units, which behave as individual singlet NGs, preserving the magnetic integrity of monomers while polymerizing.

Results and discussion

For the synthesis of dibenzo[*hi*,*st*]ovalene (DBOV) bearing two 2,6-dimethylphenyl and two phenyl groups as the precursor (**DBOV-Ph**, Fig. 1), dibrominated DBOV (**DBOV-Br**) was initially prepared through 10 synthetic steps following our previously reported procedure.[49] Then, the Suzuki coupling of **DBOV-Br** and phenyl-boronic acid provided **DBOV-Ph** in 53% yield (see Fig. 1a and methods). To explore its on-surface reactions, a submonolayer coverage of **DBOV-Ph** was sublimed onto a pristine Au(111) surface held at room temperature, followed by annealing to 200 °C. The STM image in Fig. 1b shows a rhomboid-like nanostructures formed on the metal surface. The chemical nature of the observed nanostructures was further inspected by constant-height STM and nc-AFM measurements acquired with a CO-functionalized tip (Fig. 1c and d), which demonstrate the successful formation of dibenzo[5,4]rhombene **1**, confirming the oxidative ring-closure and cyclodehydrogenation of the precursors, as well as its planar adsorption geometry.

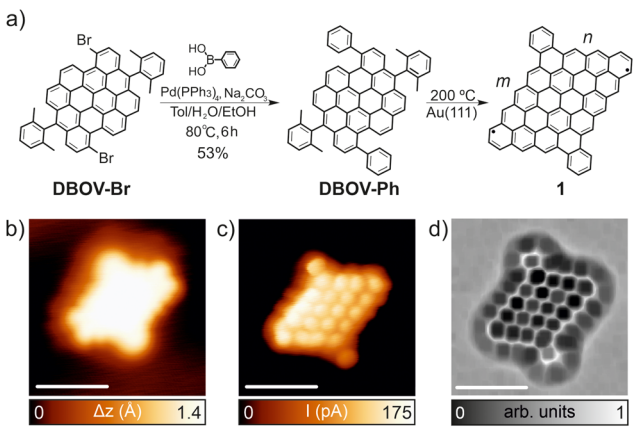

Fig. 1 Chemical structural characterization of **1** synthesized on Au(111). (a) Solution and on-surface synthesis sketch of **1** reported in this work. (b and c) Constant-current and constant-height STM images of an individual NG **1**. Scanning parameters: (b) V_b = −0.8 V, I_t = 400 pA. (c) Open feedback parameters, V_b = 5 mV, I_t = 50 pA. (d) Laplace-filtered constant-height frequency-shift nc-AFM image of **1** acquired with a CO-functionalized tip (z-offset 170 pm above the STM set point at 5 mV, 50 pA). All scale bars = 1 nm.

Next, we have investigated the electronic structure of **1**. We performed Complete-Active-Space configuration interaction (CAS-CI) and N-electron valence state perturbation theory (NEVPT2) calculations (see Fig. S1† for the corresponding active space and Fig. S2† for the resulting many-body wavefunctions). For the freestanding NGs, this reveals an open-shell singlet ground state, with the triplet being higher in energy by 215 meV. The open-shell character of the molecule is reflected both in the spin-density at the DFT level and in the natural orbitals and their corresponding occupations at the many-body level (see Fig. S3 and 4,† respectively, and theory methods). To confirm such theoretical predictions, we performed STS measurements. Fig. 2a shows the experimental long-range differential conductance dI/dV spectra of **1** featuring a series of peaks in the local density of states (LDOS) assigned to the PIR−1 (−700 mV, PIR = positive ion resonance), PIR (−350 mV), NIR (800 mV, NIR = negative ion resonance) and NIR+1 (1300 mV). Thus, the experimental Coulomb gap of **1** was found to be 1150 meV, established on the basis of the energies of the PIR and NIR resonances. To analyze the dI/dV maps of the frontier molecular orbitals for **1**, exhibiting a strong multireference character, we employed the concept of Dyson orbitals, which are defined as overlaps between the many-body wavefunctions of the neutral and charged molecules, thereby explicitly accounting for both the positive and negative molecular ions (refer to the theoretical section and Fig. S5†).[50] The experimental dI/dV maps (top row of Fig. 2b) recorded at the energy position of the ion resonances shown in Fig. 2a reveal a good agreement with the calculated Dyson orbitals corresponding to single electron additions (NIR and NIR+1) and electron removal (PIR and PIR−1) from the singlet ground state (bottom row of Fig. 2b), altogether ratifying our rationalization of the electronic structure of **1**.

Interestingly, an indirect indication of the magnetic ground state of **1** is manifested in the dI/dV spectra acquired in the vicinity of the Fermi level (Fig. 2c) which shows two conductance steps symmetrically positioned around the Fermi energy, assigned to inelastic excitations. Through d^2I/dV^2 spectroscopy, the precise energetic positions of the steps are determined, revealing an experimental singlet–triplet spin–flip excitation energy, or MEC parameter, of J_{eff} = 193 meV (in reasonable agreement with the 215 meV singlet–triplet gap predicted by NEVPT2). This experimental value is ≈10 meV larger compared to the [5,4]rhombene with a MEC of 183 meV, and slightly higher than the previous MEC record of NG on the Au (111) surface,[27] which is often desirable for enhancing the robustness of the magnetic ground state.[44] Herein, it is noteworthy to mention that while the observed step-like features in dI/dV may also originate from vibrational modes, the agreement between the experimentally determined excitation energy and the singlet–triplet gap predicted by NEVPT2 calculations strongly supports their assignment to magnetic spin–flip exci-

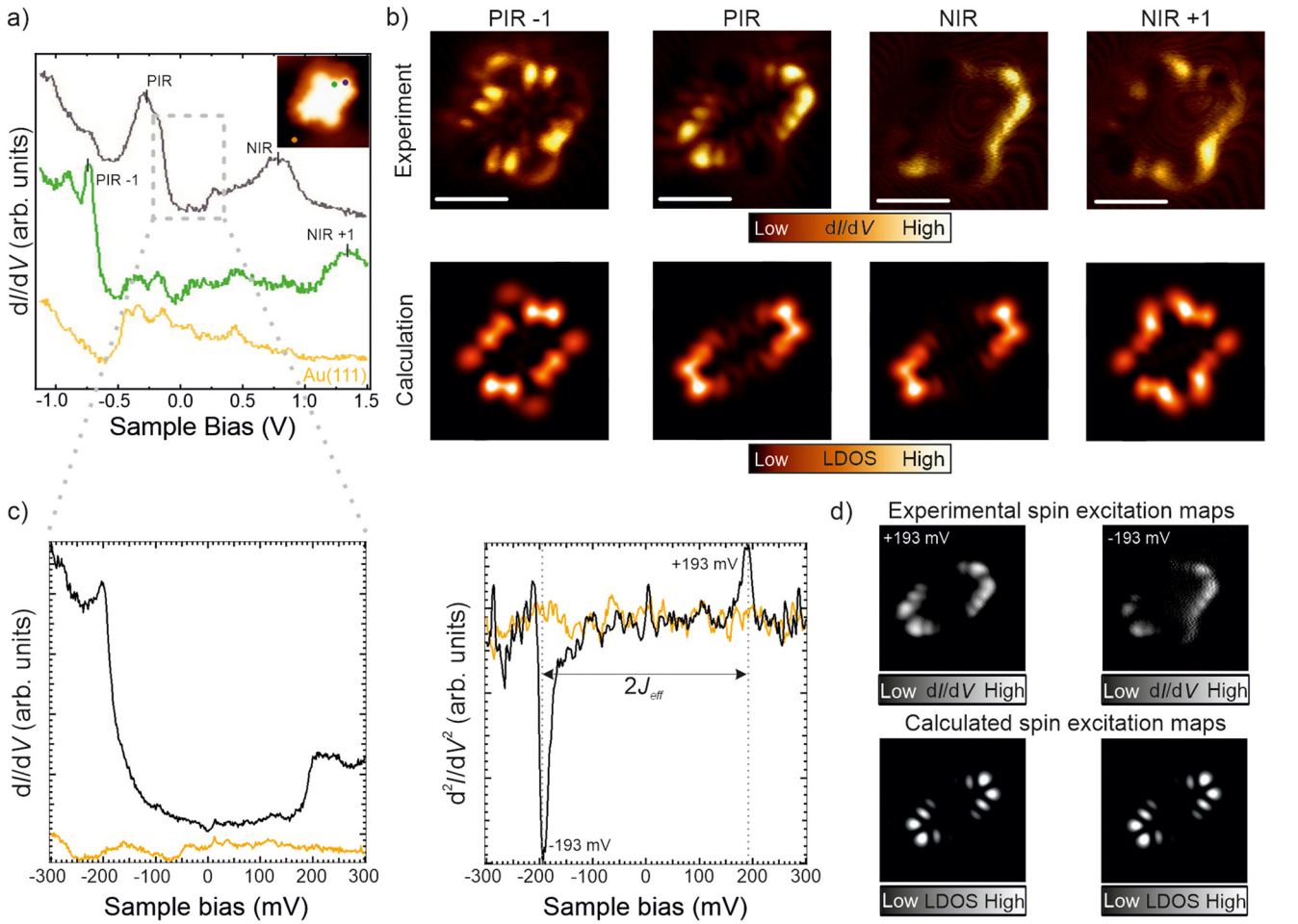

Fig. 2 Electronic characterization of **1**. (a) Differential conductance spectra of the molecule acquired with a CO-functionalized tip; black, green and orange curves were acquired at the positions indicated in the constant-current STM image (V_b = 1 V, I_t = 40 pA) in the inset. (b) Experimental constant-current differential conductance maps (top) at the energetic positions corresponding to the frontier orbitals marked in (a), and Dyson orbitals of the corresponding electron system in the gas phase (bottom). d*I*/d*V* map parameters: PIR–1 (V_b = −0.7 V, I_t = 400 pA), PIR (V_b = −0.25 V, I_t = 400 pA), NIR (V_b = 0.8 V, I_t = 400 pA) and NIR+1 (V_b = 1.3 V, I_t = 400 pA). All scale bars = 1 nm. (c) Short-range differential conductance spectra and the corresponding inelastic electron tunneling spectroscopy (IETS) spectra where the J_{eff} value for **1** is defined. Open feedback parameters, V_b = 300 mV, I_t = 650 pA, V_{rms} = 3 mV. The acquisition positions for the spectra are the ones indicated by black and orange colors on (a). (d) Inelastic spin excitation d*I*/d*V* maps acquired at V_b = ±193 mV, I_t = 400 pA, V_{rms} = 1 mV and corresponding simulated maps from the singlet–triplet Natural Transition Orbitals of **1**.

tations. In addition, the constant-current d*I*/d*V* maps obtained close to the spin excitation thresholds are shown in Fig. 2d, in agreement with the calculated Natural Transition Orbitals corresponding to the singlet–triplet excitation (see Fig. S6†) to account for the spatial resolution of the IETS signal, further confirming the singlet ground state of **1**. Since the molecule possesses diradical character, the spin signal (see Fig. 2d) coincides to some degree with the ion resonances in which the radicals are present (compare Fig. 2b).

Moreover, we have explored the intermolecular carbon–carbon coupling of **1** using functionalized precursors, **DBOV-Ph-Br** and **DBOV-Ph-iPr**, equipped with bromine and isopropyl functional groups, respectively (Fig. 3a), which were synthesized in a similar manner as **DBOV-Ph** (see the ESI† for details). Annealing at 250 °C a sample containing **DBOV-Ph-Br** or **DBOV-Ph-iPr** affords the expected oxidative ring closure and dehydrogenation reactions, along with the Ullman-like coupling[51] and the [3 + 3] cycloaromatization of isopropyl substituents, respectively,[15,52,53] towards molecular chains consisting of dibenzo[5,4]rhombene moieties that are directly coupled or conjugated with phenylene linkers.

Fig. 3b,c show high-resolution constant-current (top) and constant-height (bottom) STM images acquired with a CO-functionalized tip, confirming our assumptions for both chemical reactions, with distances between NG units of 1.8 (**2**) and 2.2 nm (**3**), respectively. Furthermore, STS measurements performed on different positions of both chains reveal similar features as those observed for **1** (Fig. 3c), which points toward a lack of interaction between closest spins of adjacent nanographene units (see Fig. S7† for a different

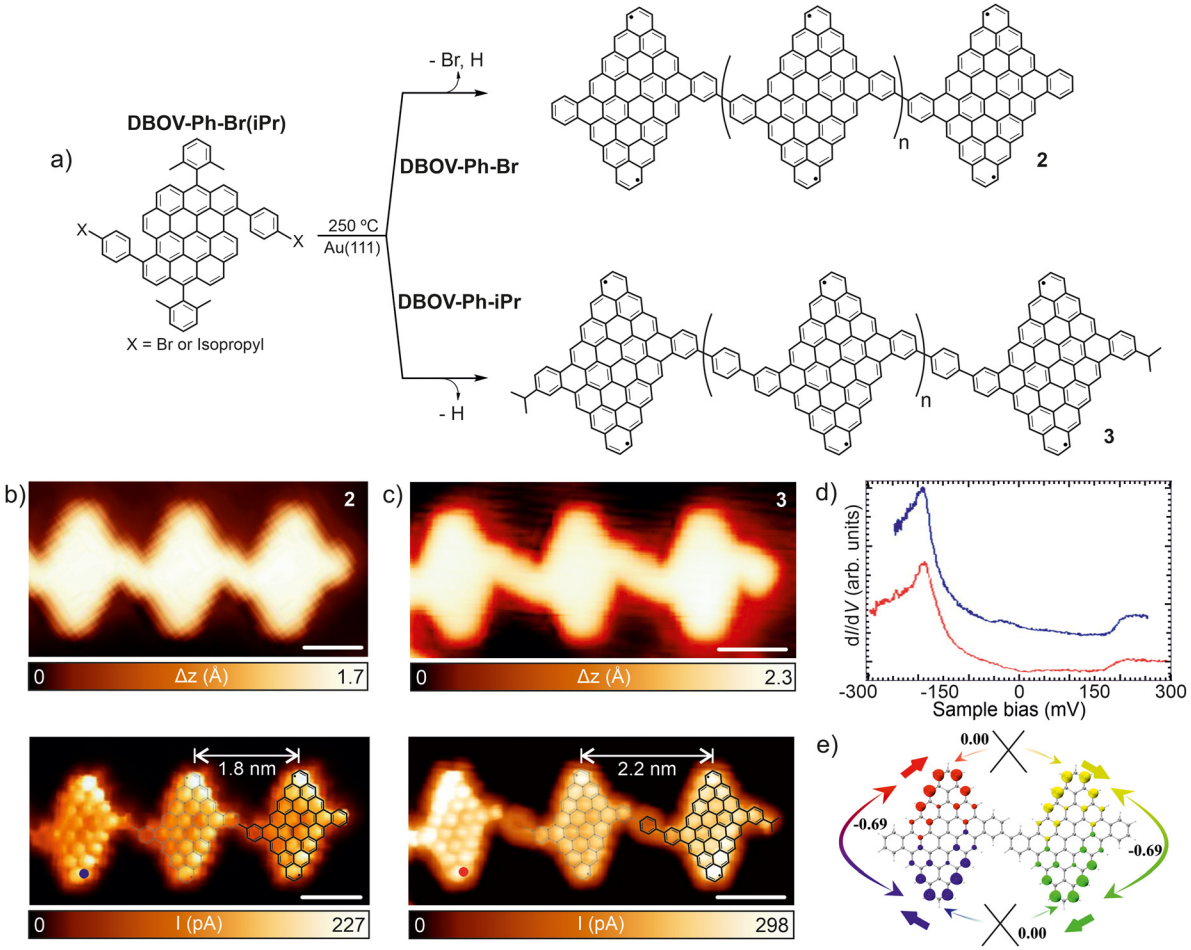

Fig. 3 Synthesis of one-dimensional chains with **1** as repeating unit. (a) Chemical sketch of the two molecular precursors (**DBOV-Ph-Br** and **DBOV-Ph-iPr**) deposited on the Au(111) surface to induce the formation of 1D chains through carbon–carbon couplings. (b and c) High-resolution constant-current and constant-height STM images of 1D chains with **1** as a repeating unit acquired with a CO-functionalized tip, together with the corresponding sketches. In (b) units of **1** are connected through single carbon–carbon bonds through the Ullmann-like reaction of the **DBOV-Ph-Br** precursor, while in (c) the linking units are benzene rings, coming from the [3 + 3] cycloaromatization of isopropyl of the **DBOV-Ph-iPr** precursor. Open feedback parameters, V_b = 5 mV, I_t = 50 pA. All scale bars = 1 nm. (d) Short-range STS measurements performed at the positions marked with blue and red colored circles in (b) and (c), respectively. Open feedback parameters; blue curve: V_b = 250 mV, I_t = 300 pA, V_{rms} = 3 mV, red curve: V_b = 300 mV, I_t = 500 pA, V_{rms} = 3 mV. (e) Representation of the spin correlations for a dimer **3**. The spins on the same NG unit have an antiferromagnetic coupling with a spin correlation of −0.69, while the spin correlation between the adjacent sites are zero, indicating that they are independent units.

coupling motif and its corresponding STS measurements). This result suggests that the dibenzo[5,4]rhombene moieties in these chains behave as isolated π-magnetic units for the explored configurations and NG distances, in agreement with the many-body calculations, where the spin-correlations in the localized orbitals (shown in Fig. S8 and 9†) calculated between neighboring spins in adjacent monomers is zero, allowing for independent spin states (see theoretical section and Fig. 3e). This behavior contrasts with the formation of a collective spin system observed in other reported cases.[37–39,42,43] Nonetheless, future experiments varying the proximity of **1** units through distinct synthetic strategies will be performed to get further insights into the magnetic characteristics of this NG.

Conclusions

In summary, we have demonstrated the synthesis of the dibenzo[5,4]rhombene featuring a strong MEC for a NG synthesized on an Au(111) surface under UHV conditions, resulting from the net spin polarization of its edge states. The chemical structure of **1** was characterized using STM and nc-AFM. STS measurements, supported by advanced theoretical calculations, revealed the electronic and magnetic properties of **1**, including its Coulomb gap of 1.15 eV and the open-shell singlet ground state, which was evidenced by singlet–triplet inelastic excitations with a J_{eff} = 193 meV.

Furthermore, we explored the fabrication of molecular chains consisting of **1** with different periodicities *via* homo-

coupling using bromo- and isopropyl-functionalized precursors, revealing a lack of intra-chain MEC between adjacent NG units (**2** and **3**). Each unit behaves as an individual antiferromagnetic NG, providing important insights into the behavior of open-shell systems and their fundamental magnetic interactions. This work contributes to the broader understanding of spin polarization in nanographenes and offers a valuable framework for future developments in molecular spintronics and quantum materials.

Author contributions

J. I. U., A. N., P. J. and D. E. conceived the idea of this study. A. B., E. P, A. P. S and A. G. performed the experimental measurements. G. and Z. G. did the solution synthesis of the precursors. M. K. and D. S. performed the theoretical calculations. J. I. U., K. L. and A. B. analyzed the data. E. P, A. P. S, A. G., J. M. G. and R. M. contributed to the data analysis. J. I. U., A. N. and P. J. wrote the manuscript. All authors participated in the manuscript preparation.

Conflicts of interest

There are no conflicts to declare.

Data availability

Data for this article, including DFT, STS and STM images are available at repositorio institucional Imdea Nanociencia at **https://repositorio.imdeananociencia.org/home**.

Acknowledgements

The authors acknowledge different funding organizations for their financial support. We thank support from the TEC-2024/TEC-459-(SINMOLMAT-CM) and '(MAD2D-CM)-IMDEA-Nanociencia' projects funded by Comunidad de Madrid, by the Recovery, Transformation and Resilience Plan, and by NextGenerationEU from the European Union, and from the Spanish Ministry of Science, Innovation and Universities (Project PID2022-136961NB-I00 and PID2023-152793NA-I00). IMDEA Nanociencia also acknowledges the "Severo Ochoa" Programme for Centers of Excellence in R&D (MINECO, Grant SEV-2016-0686 and CEX2020-001039-S). We are grateful to support by the Okinawa Institute of Science and Technology Graduate University, JSPS International Joint Research Program (JRP-LEAD with DFG) No. JPJSJRP20221607, and JSPS KAKENHI Grant No. JP22F22031. G. acknowledges the JSPS Postdoctoral Fellowship for Research in Japan. We appreciate funding from the Praemium Academie of the Academy of Science of the Czech Republic and the CzechNanoLab Research Infrastructure supported by MEYS CR (LM2018110). P.J. thanks the support of the GACR 23-05486S. J.I.U. and A.B. acknowledge the funding from MCIU for the Ramón y Cajal (RYC2022-037352) and Juan de la Cierva (FJC2021-046524-I) programs, respectively.

References

1 S. Song, J. Su, M. Telychko, J. Li, G. Li, Y. Li, C. Su, J. Wu and J. Lu, *Chem. Soc. Rev.*, 2021, **50**, 3238–3262.
2 Y. Zhang, B. Fu, N. Li, J. Lu and J. Cai, *Chem. – Eur. J.*, 2024, **30**, e202402765.
3 J. Su, P. Lyu and J. Lu, *Precis. Chem.*, 2023, **1**, 565–575.
4 S. N. Datta, A. K. Pal and A. Panda, *Chem. Phys. Impact*, 2023, **7**, 100379.
5 D. G. De Oteyza and T. Frederiksen, *J. Phys.: Condens. Matter*, 2022, **34**, 443001.
6 H. González-Herrero, J. I. Mendieta-Moreno, S. Edalatmanesh, J. Santos, N. Martín, D. Écija, B. de la Torre and P. Jelinek, *Adv. Mater.*, 2021, **33**, 2104495.
7 M. Stępień, E. Gońka, M. Żyła and N. Sprutta, *Chem. Rev.*, 2017, **117**, 3479–3716.
8 C. Zhang, Z. Yi and W. Xu, *Mater. Futures*, 2022, **1**, 032301.
9 S. Mishra, D. Beyer, K. Eimre, S. Kezilebieke, R. Berger, O. Gröning, C. A. Pignedoli, K. Müllen, P. Liljeroth, P. Ruffieux, X. Feng and R. Fasel, *Nat. Nanotechnol.*, 2020, **15**, 22–28.
10 E. Turco, A. Bernhardt, N. Krane, L. Valenta, R. Fasel, M. Juríček and P. Ruffieux, *JACS Au*, 2023, **3**, 1358–1364.
11 T. Wang, A. Berdonces-Layunta, N. Friedrich, M. Vilas-Varela, J. P. Calupitan, J. I. Pascual, D. Peña, D. Casanova, M. Corso and D. G. de Oteyza, *J. Am. Chem. Soc.*, 2022, **144**, 4522–4529.
12 J. Li, S. Sanz, J. Castro-Esteban, M. Vilas-Varela, N. Friedrich, T. Frederiksen, D. Peña and J. I. Pascual, *Phys. Rev. Lett.*, 2020, **124**, 177201.
13 X. Su, C. Li, Q. Du, K. Tao, S. Wang and P. Yu, *Nano Lett.*, 2020, **20**, 6859–6864.
14 Q. Sun, L. M. Mateo, R. Robles, P. Ruffieux, N. Lorente, G. Bottari, T. Torres and R. Fasel, *J. Am. Chem. Soc.*, 2020, **142**, 18109–18117.
15 K. Biswas, M. Urbani, A. Sánchez-Grande, D. Soler-Polo, K. Lauwaet, A. Matěj, P. Mutombo, L. Veis, J. Brabec, K. Pernal, J. M. Gallego, R. Miranda, D. Écija, P. Jelínek, T. Torres and J. I. Urgel, *J. Am. Chem. Soc.*, 2022, **144**, 12725–12731.
16 A. Sánchez-Grande, J. I. Urgel, L. Veis, S. Edalatmanesh, J. Santos, K. Lauwaet, P. Mutombo, J. M. Gallego, J. Brabec, P. Beran, D. Nachtigallová, R. Miranda, N. Martín, P. Jelínek and D. Écija, *J. Phys. Chem. Lett.*, 2021, **12**, 330–336.
17 K. Biswas, J. I. Urgel, M. R. Ajayakumar, J. Ma, A. Sánchez-Grande, S. Edalatmanesh, K. Lauwaet, P. Mutombo, J. M. Gallego, R. Miranda, P. Jelínek, X. Feng and D. Écija, *Angew. Chem., Int. Ed.*, 2022, **61**, e202114983.
18 A. Sánchez-Grande, J. I. Urgel, A. Cahlík, J. Santos, S. Edalatmanesh, E. Rodríguez-Sánchez, K. Lauwaet,

P. Mutombo, D. Nachtigallová, R. Nieman, H. Lischka, B. Torre, R. Miranda, O. Gröning, N. Martín, P. Jelínek and D. Écija, *Angew. Chem., Int. Ed.*, 2020, **59**, 17594–17599.

19 E. Turco, S. Mishra, J. Melidonie, K. Eimre, S. Obermann, C. A. Pignedoli, R. Fasel, X. Feng and P. Ruffieux, *J. Phys. Chem. Lett.*, 2021, **12**, 8314–8319.

20 Z. Ruan, J. Schramm, J. B. Bauer, T. Naumann, L. V. Müller, F. Sättele, H. F. Bettinger, R. Tonner-Zech and J. M. Gottfried, *J. Am. Chem. Soc.*, 2025, **147**, 4862–4870.

21 Q. Du, X. Su, Y. Liu, Y. Jiang, C. Li, K. Yan, R. Ortiz, T. Frederiksen, S. Wang and P. Yu, *Nat. Commun.*, 2023, **14**, 4802.

22 A. Vegliante, S. Fernández, R. Ortiz, M. Vilas-Varela, T. Y. Baum, N. Friedrich, F. Romero-Lara, A. Aguirre, K. Vaxevani, D. Wang, C. García-Fernández, H. S. J. van der Zant, T. Frederiksen, D. Peña and J. I. Pascual, *ACS Nano*, 2024, **18**, 26514–26521.

23 D. Li, O. J. Silveira, T. Matsuda, H. Hayashi, H. Maeda, A. S. Foster and S. Kawai, *Angew. Chem., Int. Ed.*, 2024, **63**, e202411893.

24 K. Biswas, Q. Chen, S. Obermann, J. Ma, D. Soler-Polo, J. Melidonie, A. Barragán, A. Sánchez-Grande, K. Lauwaet, J. M. Gallego, R. Miranda, D. Écija, P. Jelínek, X. Feng and J. I. Urgel, *Angew. Chem.*, 2024, **136**, e202318185.

25 Y. Zheng, C. Li, Y. Zhao, D. Beyer, G. Wang, C. Xu, X. Yue, Y. Chen, D.-D. Guan, Y.-Y. Li, H. Zheng, C. Liu, W. Luo, X. Feng, S. Wang and J. Jia, *Phys. Rev. Lett.*, 2020, **124**, 147206.

26 S. Mishra, X. Yao, Q. Chen, K. Eimre, O. Gröning, R. Ortiz, M. Di Giovannantonio, J. C. Sancho-García, J. Fernández-Rossier, C. A. Pignedoli, K. Müllen, P. Ruffieux, A. Narita and R. Fasel, *Nat. Chem.*, 2021, **13**, 581–586.

27 K. Biswas, D. Soler, S. Mishra, Q. Chen, X. Yao, A. Sánchez-Grande, K. Eimre, P. Mutombo, C. Martín-Fuentes, K. Lauwaet, J. M. Gallego, P. Ruffieux, C. A. Pignedoli, K. Müllen, R. Miranda, J. I. Urgel, A. Narita, R. Fasel, P. Jelínek and D. Écija, *J. Am. Chem. Soc.*, 2023, **145**, 2968–2974.

28 K. Biswas, L. Yang, J. Ma, A. Sánchez-Grande, Q. Chen, K. Lauwaet, J. M. Gallego, R. Miranda, D. Écija, P. Jelínek, X. Feng and J. I. Urgel, *Nanomaterials*, 2022, **12**, 224.

29 Y. Zheng, C. Li, C. Xu, D. Beyer, X. Yue, Y. Zhao, G. Wang, D. Guan, Y. Li, H. Zheng, C. Liu, J. Liu, X. Wang, W. Luo, X. Feng, S. Wang and J. Jia, *Nat. Commun.*, 2020, **11**, 6076.

30 S. Cheng, Z. Xue, C. Li, Y. Liu, L. Xiang, Y. Ke, K. Yan, S. Wang and P. Yu, *Nat. Commun.*, 2022, **13**, 1705.

31 S. Song, A. Pinar Solé, A. Matěj, G. Li, O. Stetsovych, D. Soler, H. Yang, M. Telychko, J. Li, M. Kumar, Q. Chen, S. Edalatmanesh, J. Brabec, L. Veis, J. Wu, P. Jelinek and J. Lu, *Nat. Chem.*, 2024, **16**, 938–944.

32 F. Villalobos, J. Berger, A. Matěj, R. Nieman, A. Sánchez-Grande, D. Soler, A. Pinar Solé, H. Lischka, M. Matoušek, J. Brabec, L. Veis, A. Millan, C. Sánchez-Sánchez, A. Campaña, J. Cuerva and P. Jelínek, *Chem*, 2025, **11**, 102316.

33 S. Mishra, D. Beyer, K. Eimre, J. Liu, R. Berger, O. Gröning, C. A. Pignedoli, K. Müllen, R. Fasel, X. Feng and P. Ruffieux, *J. Am. Chem. Soc.*, 2019, **141**, 10621–10625.

34 S. Mishra, D. Beyer, K. Eimre, R. Ortiz, J. Fernández-Rossier, R. Berger, O. Gröning, C. A. Pignedoli, R. Fasel, X. Feng and P. Ruffieux, *Angew. Chem., Int. Ed.*, 2020, **59**, 12041–12047.

35 C. Li, Y. Liu, Y. Liu, F.-H. Xue, D. Guan, Y. Li, H. Zheng, C. Liu, J. Jia, P.-N. Liu, D.-Y. Li and S. Wang, *CCS Chem.*, 2022, **5**, 695–703.

36 M. Vilas-Varela, F. Romero-Lara, A. Vegliante, J. P. Calupitan, A. Martínez, L. Meyer, U. Uriarte-Amiano, N. Friedrich, D. Wang, F. Schulz, N. E. Koval, M. E. Sandoval-Salinas, D. Casanova, M. Corso, E. Artacho, D. Peña and J. I. Pascual, *Angew. Chem., Int. Ed.*, 2023, **62**, e202307884.

37 Y. Zhao, K. Jiang, C. Li, Y. Liu, G. Zhu, M. Pizzochero, E. Kaxiras, D. Guan, Y. Li, H. Zheng, C. Liu, J. Jia, M. Qin, X. Zhuang and S. Wang, *Nat. Chem.*, 2023, **15**, 53–60.

38 S. Mishra, G. Catarina, F. Wu, R. Ortiz, D. Jacob, K. Eimre, J. Ma, C. A. Pignedoli, X. Feng, P. Ruffieux, J. Fernández-Rossier and R. Fasel, *Nature*, 2021, **598**, 287–292.

39 J. Hieulle, S. Castro, N. Friedrich, A. Vegliante, F. R. Lara, S. Sanz, D. Rey, M. Corso, T. Frederiksen, J. I. Pascual and D. Peña, *Angew. Chem., Int. Ed.*, 2021, **60**, 25224–25229.

40 M. C. Daugherty, P. H. Jacobse, J. Jiang, J. Jornet-Somoza, R. Dorit, Z. Wang, J. Lu, R. McCurdy, W. Tang, A. Rubio, S. G. Louie, M. F. Crommie and F. R. Fischer, *J. Am. Chem. Soc.*, 2024, **146**, 15879–15886.

41 B. Cirera, A. Sánchez-Grande, B. de la Torre, J. Santos, S. Edalatmanesh, E. Rodríguez-Sánchez, K. Lauwaet, B. Mallada, R. Zbořil, R. Miranda, O. Gröning, P. Jelínek, N. Martín and D. Ecija, *Nat. Nanotechnol.*, 2020, **15**, 437–443.

42 C. Zhao, G. Catarina, J.-J. Zhang, J. C. G. Henriques, L. Yang, J. Ma, X. Feng, O. Gröning, P. Ruffieux, J. Fernández-Rossier and R. Fasel, *Nat. Nanotechnol.*, 2024, **19**, 1789–1795.

43 C. Zhao, L. Yang, J. C. G. Henriques, M. Ferri-Cortés, G. Catarina, C. A. Pignedoli, J. Ma, X. Feng, P. Ruffieux, J. Fernández-Rossier and R. Fasel, *Nat. Mater.*, 2025, **24**, 722–727.

44 R. Landauer, *IBM J. Res. Dev.*, 1961, **5**, 183–191.

45 Z. Liu, S. Fu, X. Liu, A. Narita, P. Samorì, M. Bonn and H. I. Wang, *Adv. Sci.*, 2022, **9**, 2106055.

46 D. D. Awschalom, L. C. Bassett, A. S. Dzurak, E. L. Hu and J. R. Petta, *Science*, 2013, **339**, 1174–1179.

47 E. Coronado, *Nat. Rev. Mater.*, 2020, **5**, 87–104.

48 H. Yeo, S. Debnath, B. P. Krishnan and B. W. Boudouris, *RSC Appl. Polym.*, 2024, **2**, 7–25.

49 Q. Chen, S. Thoms, S. Stöttinger, D. Schollmeyer, K. Müllen, A. Narita and T. Basché, *J. Am. Chem. Soc.*, 2019, **141**, 16439–16449.

50 R. Zuzak, M. Kumar, O. Stoica, D. Soler-Polo, J. Brabec, K. Pernal, L. Veis, R. Blieck, A. M. Echavarren, P. Jelinek

and S. Godlewski, *Angew. Chem., Int. Ed.*, 2024, **63**, e202317091.
51 M. Lackinger, *Chem. Commun.*, 2017, **53**, 7872–7885.
52 A. Kinikar, X.-Y. Wang, M. Di Giovannantonio, J. I. Urgel, P. Liu, K. Eimre, C. A. Pignedoli, S. Stolz, M. Bommert, S. Mishra, Q. Sun, R. Widmer, Z. Qiu, A. Narita, K. Müllen, P. Ruffieux and R. Fasel, *ACS Nanosci. Au*, 2024, **4**, 128–135.
53 A. Kinikar, M. Di Giovannantonio, J. I. Urgel, K. Eimre, Z. Qiu, Y. Gu, E. Jin, A. Narita, X.-Y. Wang, K. Müllen, P. Ruffieux, C. A. Pignedoli and R. Fasel, *Nat. Synth.*, 2022, **1**, 289–296.